Accepted Manuscript

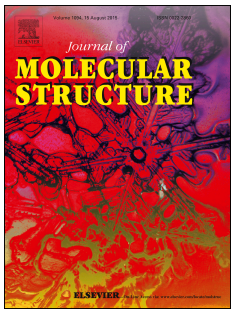

Synthesis, Click reaction, Molecular structure, Spectroscopic and DFT computational studies on 3-(2,6-bis(trifluoromethyl)phenoxy)-6-(prop-2-yn-1-yloxy)phthalonitrile

Muhammad Hasan, Mona Shalaby

PII: S0022-2860(16)30078-3

DOI: 10.1016/j.molstruc.2016.01.078

Reference: MOLSTR 22194

To appear in: *Journal of Molecular Structure*

Received Date: 15 October 2015

Revised Date: 27 January 2016

Accepted Date: 27 January 2016

Please cite this article as: M. Hasan, M. Shalaby, Synthesis, Click reaction, Molecular structure, Spectroscopic and DFT computational studies on 3-(2,6-bis(trifluoromethyl)phenoxy)-6-(prop-2-yn-1-yloxy)phthalonitrile, *Journal of Molecular Structure* (2016), doi: 10.1016/j.molstruc.2016.01.078.

Synthesis, Click reaction, Molecular structure, Spectroscopic and DFT computational studies on 3-(2,6-bis(trifluoromethyl)phenoxy)-6-(prop-2-yn-1-yloxy)phthalonitrile

Muhammad Hasan* and Mona Shalaby

Department of Chemistry, Kuwait University, P.O. Box 5969, Safat 13060, Kuwait

KEYWORDS Fluorinated phthalonitrile, FT-IR, FT-Raman, ^{13}C and ^{1}H NMR, Click chemistry, and DFT.

* Corresponding author. Tel.: +96599686945; fax: +96524816482.
E-mail address: m.hasan@ku.edu.kw.

ABSTRACT:

The compound 3-(2,6-bis(trifluoromethyl)phenoxy)-6-(prop-2-yn-1-yloxy)phthalonitrile has been synthesized and confirmed by different characterization techniques such as elemental analysis, IR, UV-vis spectroscopy, and X-ray single-crystal determination. The molecular geometry from X-ray determination of this compound in the ground state has been compared using the Hartree-Fock (HF) and density functional theory (DFT) with the 6-31G(d) basis set. This compound reacted with sugar azide via click reaction to form triazol ring. The synergy between carbohydrate molecule and fluorinated organic compound achieved novel synthetic pathways, properties, and applications in chemistry science.

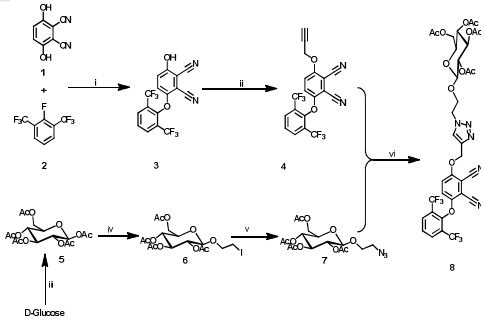

Introduction

Phthalonitrile is considered as petals of a dye molecule which form a ring around an atom to create a flower-like dye molecule called phthalocyanine.[1] This unique reaction is but one of the fascinating properties that make phthalonitrile so promising for producing an important class of molecules with various application possibilities in sensors, catalysis, non-linear optics (NLO), optical data storage, photodynamic cancer therapy (PDT), bio-imaging and nanotechnology .[2-5] These leads to developments of new synthetic efforts for enlarge the access to new derivatives.

The insertion of fluorine atom to the phthalocyanine precursor may enrich the pharmacokinetic features, lipophilicity, and high level of singlet oxygen production and selective accumulation of photosensitizer in tumor cells which make from this photosensitizer potential entity for photodynamic therapy. Noteworthy, the fluorinated compounds possess a remarkable magnetic resonance which constitutes excellent probe for sensitive and minimally invasive imaging. [6] Unfortunately, the initial attempts for synthesizing di-substituted phthalonitrile didn't succeed and gave only a monosubstituted phthalonitrile. In order to overcome this problem, a terminal alkyne was prepared to represent a new building block for further preparation of versatile functionalized phthalonitriles. Superior combination of fluorine substituents with other functional groups in their structures, such as sugars led to novel molecules possessing outstanding phototoxicity in both in vitro and in vivo studies. [6]

The Huisgen 1,3-dipolar cycloaddition reaction of organic azides and alkynes has gained considerable attention in recent years due to the using of Cu(1) as a catalyst by Tornøe and Meldal,[7, 8] leading to a major improvement in both rate and regioselectivity for the click reaction.[9, 10] Huisgen click reaction is using here to functionalize phthalonitrile with sugar molecule. Two advantages could appears from functionalizing the photosensitizers with carbohydrates substituent, in addition to water-solubility: a potential selective recognition by the targeting cancer cells and an increased uptake due to the high energy requirements of cancer cells that consume much more carbohydrate than other cells, as it is a readily available energy source.[11] In recent years, density functional theory (DFT) has been a shooting star in theoretical modeling. Many important chemical and physical properties of

biological and chemical systems can be predicted by various computational techniques.[12]

Vibrational studies for the precursor molecules are considered important and extremely valuable when performing these studies on larger composite molecular Systems. [13]

In this paper, we designed fluorinated phthalonitrile with terminal alkyne and grafted by carbohydrate azide. This phthalonitrile can used for the preparation of unsymmetrical phthalocyanines, which has become the focus of interest [14] as well as the theoretical studies on the phthalonitrile with terminal alkyne by using the HF/6-31G(d) and DFT/B3LYP/6-31G(d) methods.

Experimental and theoretical methods

General Procedures. Among the starting materials, 2,3-Dicyano-1,4-hydroquinone, 2,6-Bis-(trifluoromethyl)fluorobenzene, 1,4-dihydroxynaphthalene-2,3-dicarbonitrile, 3-Bromoprop-1-yne 80% w/w in toluene were purchased from Sigma-Aldrich, Matrix Scientific and Alfa Aesar and used directly without further purification. Sugar azide was synthesized according to the literature method.[15-17] TLC was performed using Polygram sil G/UV 254 TLC plates and visualization was carried out by ultraviolet light at 254 nm and 350 nm. Column chromatography was performed using Merck silica gel 60 of mesh size 0.040–0.063 mm. Anhydrous solvents were either supplied from Sigma-Aldrich and used as they were received or dried as described by Perrin. [18] The ^{1}H NMR and ^{13}C NMR Spectra (400 MHz) were recorded using Bruker DPX 400 and IR spectra were obtained from Jasco 6300 FTIR. UV–Vis studies were done on a Varian Cary 5 spectrometer and Shimadzu UV-2401Pc spectrophotometer. Elemental analyses were carried out using Elementar Vario Micro Cube. Mass analyses were done by electron impact (EI) on a Thermo DFS mass spectrometer. A high resolution mass analysis (HRMS) was measured on Xevo G2-S QTof. Differential scanning calorimetry (DSC) analyses were carried out on Shimadzu DSC-50. Single crystal data collections were made on a Bruker X8 Prospector using filtered Cu- Kα radiation. The diffraction data were collected at room temperature. Raman spectra and images were obtained using a confocal microprobe Raman system (Invia, Renishaw). Ar laser (514 nm) was used for compound (**4**) and Diode (Semi-conductor) laser (785 nm) for compound (**8**) for the Raman measurement. The laser power at the sample was 10% for compound (**4**) and 100% for compound (**8**). Typical exposure time for cell measurement was 20 s for compound (**4**) and 1 s for compound (**8**). The laser spot was focused on the sample surface using a long working distance x100 objective. Raman spectra were collected on numerous spots on the sample and recorded with Renishaw CCD camera.

Syntheses.

3-(2,6-bis(trifluoromethyl)phenoxy)-6-hydroxyphthalonitrile (3) To a stirred solution of 2,3-Dicyano-1,4-hydroquinone (**1**, 1gm, 6.2 mmol) and anhydrous potassium carbonate (4.3 gm, 5 equiv) in dry N-Methyl-2-pyrrolidone (NMP) under nitrogen atmosphere, 2,6-Bis-(trifluoromethyl)fluorobenzene (**2**, 1.4 gm, 1 equiv) was added drop wisely. The reaction mixture was heated at 130 °C for 24 h. Then after being cooled, it was poured into acidic distilled water and the resulting precipitate was collected by filtration and washed several times with distilled water, then dry in oven and recrystallized by Ethyl acetate (EA)/ n-hexane to give white crystals yield (1 gm, 58.82 %). Mp: 219.9 °C; IR (KBr) ν/cm^{-1}: 3277.43 (OH), 2251.49 (CN); ^{1}HNMR (400 MHz, DMSO), δ/ppm: 6.97 (1H, d, H_{ar}); 7.23(1H, d, H_{ar}); 7.83(1H, t, H_{ar}); 8.26(2H, d, H_{ar}); 11.85(1H, br, OH). ^{13}C NMR (DMSO), δ/ppm: 156.95 (O-C-Ar); 153.09 (O-C-Ar); 147.57 (O-C-Ar); 133.01 ,132.98, 132.95, 132.91 (C-Ar); 128.51 (C-CF_3); 124.96 (C-Ar); 124.80, 124.59, 124.38, 124.16 (CF_3); 123,41, 123.15 (C-Ar) ; 121.90, 121.34 (C-Ar) ; 113.62, 112.69 (C≡N); 102.14, 100.52 (C*-CN). Anal. Calcd (%) for $C_{16}H_6F_6N_2O_2$: C 51.63; H 1.62; N 7.53. Found: C 51.77; H 1.71; N 7.55.

3-(2,6-bis(trifluoromethyl)phenoxy)-6-(prop-2-yn-1-yloxy)phthalonitrile (4) to a solution of 3-(2,6-bis(trifluoromethyl)phenoxy)-6-hydroxyphthalonitrile (**3**, 1 gm, 2.6 mmol) in dry acetone (20 ml) anhydrous potassium carbonate (K_2CO_3, 1.8 gm , 5 equiv) was added, and the mixture was refluxed, then propagyl bromide (1 ml) was added drop by drop while refluxing. The resulting mixture was stirred and refluxed for 20 h. the mixture was cooled and evaporated under vacuum and then add water with stirring then filter. The crude product was purified with column chromatograph on silica gel eluted with Dichloromethane (DCM): n-hexane (3:5, v/v) to give a white ppt, which was recrystallized by DCM/ n-hexane. Yield: (0.8 gm , 72.72 %). Mp: 151.2 °C; IR (KBr) ν/cm^{-1}: 3300(C≡C-H),3083.62, 3056.62 (C-H_{ar}), 2234.13(C≡N), 2131.92 (C≡C); ^{1}HNMR (400 MHz, DMSO) δ/ppm: 8.30 (2H, d, H_{ar}); 7.87 (1H,t, H_{ar}); 7.57(1H, d, H_{ar}); 7.26(1H, d, H_{ar}); 5.08 (2H, d, CH_2), 3.75 (1H, s, HC≡C). ^{13}C NMR (DMSO), δ/ppm: 155.07 (O-C-Ar); 154.22 (O-C-Ar); 147.31 (O-C-Ar); 133.02 (C-Ar); 128.68 (C-CF_3); 124.94 (C-Ar); 124.70, 124.48, 124.27 , 124.06 (CF_3); 123.13 (C-Ar) ; 121.64, 121.31, 120.97 (C- Ar) ; 112.84, 112.25 (C≡N); 103.81, 103.28 (C*-CN); 79.99 (H-C*≡C-); 77.48 (C≡C-H); 57.71 (CH_2) ; *m/z* (EI) = 410.1 [M^{+}]; Anal. Calcd (%) for $C_{19}H_8F_6N_2O_2$: C 55.62; H 1.97; N 6.83, Found: C 55.58; H 2.07; N 6.76; TOF-ES-MS: found (m/z) 411.0583 [M+H]$^{+}$, calcd for C19H9N2O2F6 (m/z) 411.0568 [M+H]$^{+}$.

Synthesis of glucose with spacer. The synthesis protocol of the glucose spacer was performed in three steps according to literatures [15-17]

1,2,3,4,6-penta-O-acetyl-β-D-gulcopyranoside (5) was synthesized as in literature. **[15]**

(2-chloroethyl)-2,3,4,6-tetra-O-acetyl-β-D-glucopyranoside (6) was synthesized as in literature [16] with some modification. 1,2,3,4,6-penta-O-acetyl-β-D-gulcopyranoside (**5**, 5 gm, 12.8 mmol) was dissolved in 100 ml dry DCM with adding molecular sieves 4 Å (2.5 gm). 2-iodoethanol was added drop wisely to the pervious mixture with stirring at room temperature for 0.5 h. The resulting reaction mixture was cold at 0 °C in ice bath. BF3.etherate (4 ml) was added drop wisely then the reaction mixture was stirred at room temperature over night. After completion K_2CO_3 (2.37 gm) was added and allowed to stir for 5 min. Filter the salt and the reaction mixture extracted with 200 ml of water two times. DCM solution was collected and dried over anhydrous sodium sulfate, filter and then evaporated the solution. The crude product was purified using column chromatograph on silica gel eluted with EA:

n-hexane (1:1, v/v). Yield: (2.5 gm, 39.06 %). ^{1}HNMR (400 MHz, $CDCl_3$) δ/ppm: 5.42 (1H, d); 5.280 (1H, dd); 5.06 (1H, dd); 4.55 (1H, d); 4.22(1H, dd), 4.14 (2H, m), 3.954 (1H, t), 3.83 (1H, m), 3.31 (2H, m); 2.18, 2.12, 2.08, 2.01 (12H, s). *m/z* (EI) = 442.1 [M^+-OAc].

(2-azidoethyl)-2,3,4,6-tetra-O-acetyl-β-D-glucopyranoside (7) was synthesized as in literature**.** [17]

(2S,3S,5R)-2-(acetoxymethyl)-6-(2-(4-((4-(2,6-bis(trifluoromethyl)phenoxy)-2,3-dicyanophenoxy)methyl)-1H-1,2,3-triazol-1-yl)ethoxy)tetrahydro-2H-pyran-3,4,5-triyl triacetate (8) alkynylphthalonitrile (**4**, 0.4 gm, 0.975 mmol) dissolved in 20 ml chloroform then add Copper iodide(I) (1 eq, 0.185 gm) and N,N-Diisopropylethylamine (DIPEA , 6 eq, 1.67 gm) to the solution with stirring. Sugar aztide (7, 1.5 eq, 0.61 gm) was then added to the solution and refluxed overnight. After completion, the reaction mixture was washed with ammonium hydroxide solution then washed two times with water and the organic phase was collected and dried over sodium sulfate. The solution was evaporated and the crude product purified by chromatograph on silica gel eluted with EA: n-hexane (1:1, v/v). Yield: (0.2 gm, 25 %). Mp: 73.1 °C; IR (KBr) ν/cm^{-1}: 3097.12(C≡C-H), 2237.02 (C≡N), 1752.98 (C=O); ^{1}HNMR (400 MHz, DMSO) δ/ppm: 8.309 (2H, d, H_{ar}); 8.161 (1H, s, triazole-CH); 7.875 (1H, t, H_{ar}); 7.798 (1H, d, H_{ar}); 7.243 (1H, d, H_{ar}), 5.391 (1H, s), 5,229 (1H, t), 4.925 (1H, t), 4.876 (1H, d), 4.750 (1H, t), 4.598 (2H, m), 4.165(2H, m), 4.053 (2H, m), 3.971 (2H, m), 2.106, 2.002, 1.901, 1.866 (12H, 5s, 5x OC(O)CH3); *m/z* (EI) = 827.0 [M^+]; TOF-ES-MS: found (m/z) 828.1939 [M+H]$^+$, calcd for $C_{35}H_{32}N_5O_{12}F_6$(m/z) 828.1952 [M+H]$^+$.

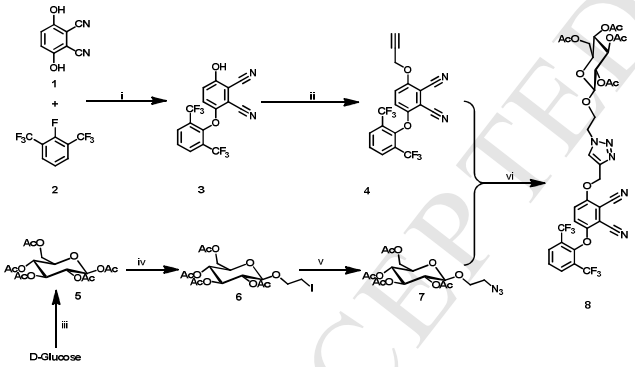

Scheme 1. Reagents and conditions. (i) NMP, anhydrous K_2CO_3, 130 °C, 24 h; (ii) acetone, propagyl bromide, anhydrous K_2CO_3, reflux, 24 h; (iii) Acetic anhydride, CH_3COONa; (iv) CH_2Cl_2, iodoethanol, $BF_3.OEt_2$; (v) DMF, NaN_3, 80°C; (vi) chloroform, CuI, reflux, 24 h.

Crystal structure determination and refinement. Single crystals of phthalonitrile **4** suitable for X-ray diffraction technique were grown by solvent diffusion method. A summary of the key crystallographic information is given in Table 1.The ball and stick representation of crystal structure derived from **4** is depicted in Fig. 1.

Computational Methods. The molecular geometry was taken directly from the X-ray diffraction experimental result without any constraints. The DFT calculations with a hybrid functional B3LYP (Becke's three parameter hybrid functional using the LYP correlation functional) with the 6-31G(d) basis set and Hatree-Fock calculations with the 6-31G(d) basis set using the Berny method[19, 20] were performed with the Gaussian 09W program. [21] The harmonic vibrational frequencies were calculated at the same level of theory for the optimized structures and the obtained frequencies were scaled by 0.9613 and 0.8929. [22] Vibrational band assignments were made using the Gauss-View molecular visualisation program. [23] The electronic absorption spectra were calculated using the time-dependent density functional theory (TD-DFT) and Hartree- Fock (TD-HF) methods [24-27] in gas phase in addition to the solvent (chloroform) effect which stimulated using the polarizable continuum model (PCM).[28-30] To investigate the reactive sites of the compound (**4**) the molecular electrostatic potential was evaluated using the B3LYP/6-31G(d) method.

For NMR calculations, after optimization, ^{1}H and ^{13}C NMR chemical shifts were calculated using the gauge-invariant atomic orbital (GIAO) method [31, 32] in DMSO. The GIAO method is one of the most common approaches for calculating nuclear magnetic shielding tensors. The GIAO approach allows the computation of the absolute chemical shielding due to the electronic environment of the individual nuclei and this method is often more accurate than those calculated with other approaches for the same basis set size. The ^{1}H and ^{13}C NMR chemical shifts were converted into the TMS scale by subtracting the calculated absolute chemical shielding of TMS the values of which are, respectively, 32.59 and 199.98 ppm for HF/6-31G(d).

Results and Discussion

Synthesis. The direct reaction between 2,3-dicyano-1,4-hydroquinone (**1**) and 2,6-Bis-(trifluoromethyl)fluorobenzene (**2**) produce mono-substituted fluorinated phthalonitrile precursor (**3**) instead of forming di-substituted fluorinated phthalonitrile as shown in scheme (1). The propargylation of phenolic hydroxyl groups using propargyl bromide through an aromatic nucleophilic substitution (SN_{Ar}) mechanism such as compound (4) is particularly important because of being a terminal alkyne moiety can be used as a prospective component for "click chemistry" along with an organic azide (**7**). Grafting carbohydrates on to this precursor via click reaction offers several advantages for the resulting photosensitiser: besides the hydrophilicity of such moieties which aids delivery in aqueous systems, potential selective recognition and enhanced cell uptake by cancer cells having elevated receptor densities for these species are possible.

Description of the Crystal Structure. The crystal structure of compound (**4**) is shown in Fig. 1a and selected bond distances and angles are summarized in Table 2. The compound (**4**) crystallizes in the monoclinic space group P 1 21/n 1 with eight molecules in the unit cell. A great attention has been focus to understand the nature of short contacts involving halogens of the type C-X...X (where X = F, Cl, Br, I) and contacts of the type C-X...O, C-X...N, and C-X...H (where X= C, N, O).[33-40] Such contacts have been known for some time in crystallographic literature, wherein

a short contact between two atoms, A and B, signifies that the distance A...B is less than the sum of the van der Waals radii.[39] Regarding the crystal structure of compound (**4**) there is short contact shown in fig. 1c. between C15...F5, N1...H3, O1...C17 and F5...H15A. This phthalonitrile linked by an O atom, forming non-planar molecular structure. The calculated torsion angles of the chain of atoms C4-O2-C15-C16 is 82.8, C1-O1-C7-C12 is 100.2, C1-O1-C7-C8 is -87.2 which confirms that the dihedral angles between the phenyl ring containing phthalonitrile functional groups are more or less 90 degrees to the plane of those phenoxy and alkynoxy substituents. The 3-dimensional packing structure of this molecule, viewing along a-, b- and c- directions are given in Fig. 2.

Table 1. Crystal data and refinement parameters for compound (4)

Formula	**C19H8F6N2O2**
Formula weight (g)	**410.27**
Temperature (K)	**296(2) K**
Wavelength	**1.54178 Å**
Crystal system	**Monoclinic**
Space group	**P 1 21/n 1**
Unit cell dimensions	
a, b, c (Å)	**7.9163(2), 18.0585(4) , 12.7302(3)**
β(°)	**90.087(2)°**
Volume ($Å^3$)	**1819.86(7)**
Z	**4**
Calculated density (g cm^{-3})	**1.497**
μ (mm^{-1})	**1.243**
F(o, o,o)	**824**
Crystal size (mm)	**0.050 x 0.150 x 0.250**
θ Ranges (°)	**4.25 - 66.38°**
Index ranges	**-9<=h<=9**
	-21<=k<=21
	-14<=l<=14
Reflections collected	**20082**
Independent reflections	**3165 [$R_{(int)}$ = 0.0427]**
Reflection observed (I > 2σ)	**2456**
Absorption correction	**multi-scan**
Refinement method	**Full-matrix least-squares on F^2**
Data/restrains/parameters	**3165 / 0 / 262**
Goodness-of-fit on F^2	**1.046**
Final R indices [Ih2r(I)]	**0.0590**
R indices (all data)	**0.0757**
Largest diff. Peak and hole (e A^{-3})	**0.417 and -0.321**

Table 2. Selected structural parameters by X-ray and theoretical calculations for compound (4)

	Experimental	**Calcd.**	
		HF	**DFT/B3LYP**
Bond lengths (Å)	1.312(7)	1.32267	1.35006
F1-C13	1.311(7)	1.31612	1.34324
F3-C13	1.308(4)	1.32443	1.35409
F5-C14	1.358(3)	1.34237	1.35836
O2-C4	1.376(3)	1.36206	1.37645
O1-C1	1.142(3)	1.13496	1.16274
N1-C18	1.158(5)	1.18600	1.20677
C17-C16	1.437(5)	1.47316	1.46422
C16-C15	0.97	1.08398	1.09869
C15-H15B	1.393(3)	1.39223	1.41017
C4-C5	1.433(3)	1.44177	1.42975
C5-C18	1.379(4)	1.38983	1.40207
C7-C12	1.362(6)	1.38200	1.39261
C10-C9	1.379(4)	1.38158	1.39270
C3-C2	0.93	1.07219	1.08362
C2-H2	1.480(6)	1.51003	1.51233
C8-C13		0.14219	0.15362
Max. difference[a]	180.0	179.455 113.347	179.223
Bond angles (°)	112.9(3)	110.435	113.756
C16-C17-H17	109.0	125.093	109.826
C16-C15-O2	126.0(2)	118.884	125.277
O2-C15-H15B	119.3(2)	119.134	119.281
O2-C4-C3	120.7(2)	119.853	119.402
C3-C4-C5	119.9(2)	120.586	119.477
C4-C5-C18	119.8(2)	115.818	120.706
C1-C6-C5	114.8(2)	119.725	115.510
C5-C6-C19	119.3(3)	120.513	119.733
O1-C1-C6	123.2(3)	119.178	120.399
C12-C7-O1	119.9	119.420	119.571
C7-C12-C14	118.9(3)	120.479	119.432
C3-C2-H2	121.6(4)	107.433	120.389
C9-C8-C7	105.5(6)	120.038	107.460
C7-C8-C13	119.8	107.404	120.470
F3-C13-F2	106.9(3)	179.711	107.435
C10-C9-H9	177.9(3)	2.717	179.765
F4-C14-F5			2.831
N1-C18-C5			
Max. difference[a]			

[a] Maximum differences between the bond lengths and angles computed using theoretical methods and those obtained from X-ray diffraction.

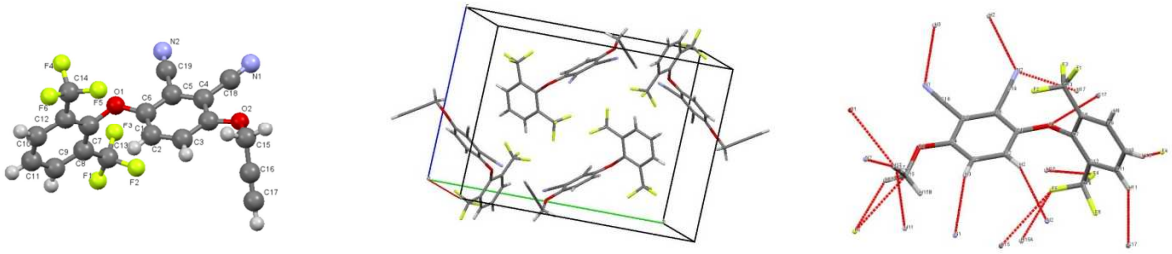

(a) **(b)** **(c)**

Fig.1. (a) The ball and stick representation of crystal structure **4**, (b) unit cell, (c) short contact

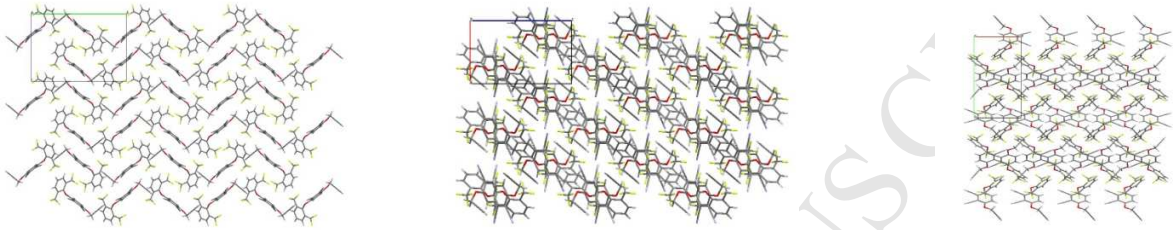

(a) (b) (c)

Fig.2. 3-dimensional packing pattern of compound (**4**) along (a) a-, (b) b- and (c) c- directions

Optimized structure

The atomic numbering scheme for the title crystal is shown in fig.1 a. B3LYP/6-31G(d) and HF/6-31G(d) calculations were performed on compound (**4**) and a selected calculated geometric parameters are listed in Table 3 along with the experimental data. The molecular structure of this compound is not planar. A superposition of the molecular structure of compounds as established by quantum mechanical calculations and X-ray study shows an excellent agreement as seen in Fig. 3. Comparing the theoretical data with the experimental ones indicates that optimized bond lengths and angle values are slightly different with the experimental results. The largest difference between experimental and calculated DFT bond length is 0.15362 Å for (C2–H2), whereas this difference for HF method is 0.14219 Å for (C2–H2), which suggest that the calculation precision is satisfactory. These theoretical results indicate that the HF method gives geometric parameters, which are much closer to experimental ones. Similar situation is also observed for calculated bond angles with HF and DFT method.

IR and Raman frequencies

IR and Raman frequencies of compound (**4**) were calculated using the DFT/B3LYP and HF methods with the 6-31G (d) basis set. The vibrational band assignments were made using the Gauss-View molecular visualisation program. Figure 4 and 5 shows the observed and calculated IR and Raman spectra of this compound. Calculated vibrational frequencies of compound (**4**) at DFT/B3LYP and HF levels were scaled by 0.96 and 0.89, respectively. [41] The experimental FT-IR spectrum of the title compound is shown in Fig. 4. The IR spectra contain some characteristic bands of the stretching vibrations of the C–H, C≡N, C≡C, C–O and CF_3 groups. The aromatic structure shows the presence of C–H stretching vibrations in the region 2900–3150 cm^{-1}, which is the characteristic region for the C–H stretching vibrations. The C-H aromatic stretching mode was observed at 3083.62 cm^{-1} experimentally, and calculated at 3087.27 cm^{-1} for B3LYP and at 3019.93 cm^{-1} for HF. The experimental C≡N stretching mode was observed at 2234.13cm^{-1} as a strong band, which have been calculated at 2258.71 cm^{-1} for B3LYP and 2330.34 cm^{-1} for HF. In the phthalonitrile, the C≡N stretching modes were observed to be 2232 - 2237cm^{-1} [13] and 2230 cm^{-1} [42] as experimentally. The C≡C stretching vibrations have a characteristic region 2100–2260cm^{-1}. The experimental C≡C stretching mode was observed at 2131.92 cm^{-1} as a weak band, which have been calculated at 2153.74 cm^{-1} for B3LYP and 2154.41 cm^{-1} for HF. The identification of C–O and CF_3 vibrations is a very difficult task, since the mixing of several bands are possible in this region. The band observed at 994.12 cm^{-1} in FT-IR spectrum is assigned to C–O stretching vibration and calculated at 977.26 cm^{-1} for B3LYP and 905.36 cm^{-1} for HF while the band observed at 1061.62 cm^{-1} in FT-IR spectrum is assigned to CF_3 stretching vibration and calculated at 1044.60 cm^{-1} for B3LYP and 1056.30 cm^{-1} for HF. It should be noted that the calculations were made for a free molecule in vacuum, while the experiments were performed for the solid samples. Moreover, two factors may be responsible for the discrepancies between the experimental and computed spectra of this compound. The first is caused by the environment and the second reason for these discrepancies is the fact that the experimental value is an anharmonic frequency while the calculated value is a

(a) (b)

Fig. 3. Atom-by-atom superimposition of the 3-(2,6-bis(trifluoromethyl)phenoxy)-6-(prop-2-yn-1-yloxy)phthalonitrile calculated a = HF (red); b = B3LYP (blue) over the X-ray structure (black).

harmonic frequency. [43, 44] In FT-Raman spectrum, the vibration mode at 2234.073 cm^{-1} is corresponding to stretching mode of C≡N group. The calculated vibration by B3LYP is 2258.88 and by HF are 2334.47 cm^{-1}. The second characteristic vibration mode at 2132.77 cm^{-1} is corresponding to stretching mode of C≡C group. The calculated vibration by B3LYP is 2155.20 cm^{-1} and by HF are 2158.25 cm^{-1}.

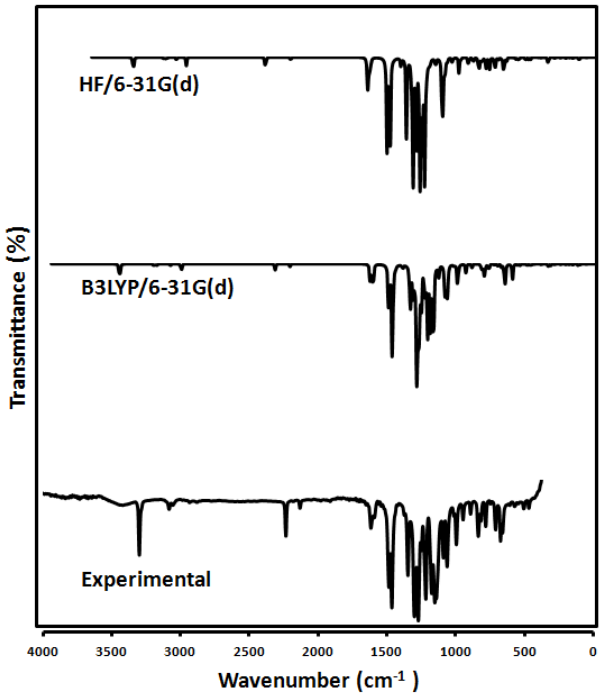

Fig.4. Observed and calculated FT-IR spectra of 3-(2,6-bis(trifluoromethyl)phenoxy)-6-(prop-2-yn-1-yloxy)phthalonitrile.

^{13}C and ^{1}H NMR calculations

The experimental ^{1}H and ^{13}C NMR spectra of compound (**4**) are shown in Fig. 6. GIAO ^{1}H and ^{13}C chemical shift values were calculated using the DFT/B3LYP method with 6-31G(d) basis set and generally compared with ^{1}H and ^{13}C chemical shift values. The calculated results are given in Table 3. ^{1}H chemical shift values are calculated to be 2.752–8.325 ppm B3LYP/6-31G(d) level, while the experimental

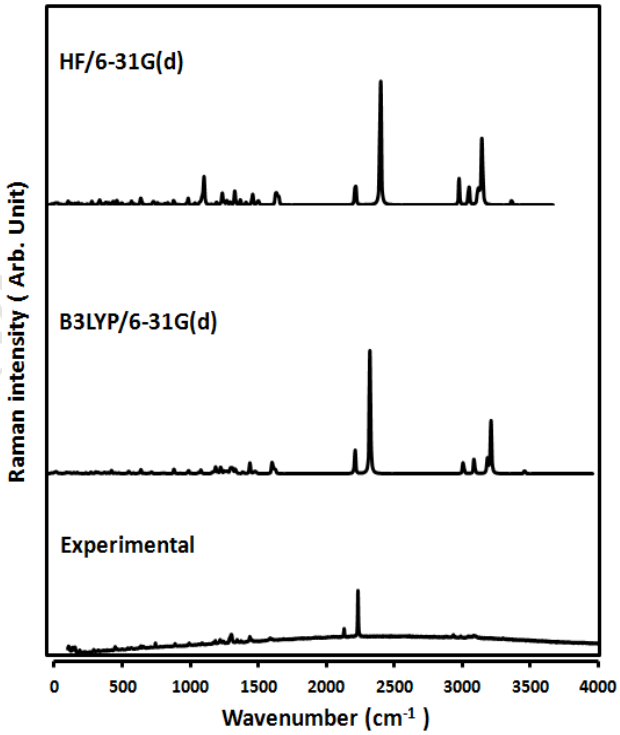

Fig.5. Observed and calculated FT-Raman spectra of 3-(2,6-bis(trifluoromethyl)phenoxy)-6-(prop-2-yn-1-yloxy)phthalonitrile.

results are observed to be 3.755–8.306 ppm. The atom positions were numbered as in Fig. 1. It is clear from Table 3 that the agreement with experimental data is good. The largest differentiation in ^{13}C chemical shifts is observed for C(13) and C(14), amounting to about 10 ppm while, the differentiation in ^{1}H NMR is observed for H(17) about 1.003 ppm . The terminal alkynyl carbons C(16) and C(17) are coupled at 77.48 and 79.99 ppm respectively, whereas the corresponding values are 77.748 and 82.288 ppm. ^{13}C NMR spectra of the compound show signals at 112.84 and 112.25 ppm due to the C(18) and C(19) atoms of the cyano groups. These signals were calculated at 115.538 and 115.257 ppm.

The chemical shift value of C(13) and C(14) atoms bounded the trifluoromethyl group is observed as quartet at 124.70 ppm, whereas the corresponding value is 135.436 and 135.465 ppm for B3LYP level. As can be seen from Table 3, the theoretical ^{1}H and ^{13}C chemical shift results for compound (**4**) are generally closer to the experimental ^{1}H and ^{13}C shift data.

Table.3 Theoretical and experimental ^{1}H and ^{13}C isotropic chemical shifts (with respect to TMS, all values in ppm) for compound (4).

Atom	Experim-ental (ppm) (DMSO)	Calculat-ed(ppm) B3LYP 6-31G(d)	Atom	Experi-mental (ppm) (DMSO)	Calculated (ppm) B3LYP 6-31G(d)
C1	155.07	161.368	H11	8.306	8.325
C4	154.22	160.168	H9	8.286	8.321
C7	147.31	152.614	H10	7.873	8.105
C11	133.02	136.980	H3	7.578	7.723
C9	133.02	136.969	H2	7.269	6.938
C14	124.70	135.465	H15B	5.081	5.410
C13	124.70	135.436	H15A	5.077	5.079
C8	128.68	133.778	H17	3.755	2.752
C12	128.68	133.767			
C10	124.94	131.838			
C2	123.13	126.439			
C3	121.64	123.886			
C18	112.84	115.538			
C19	112.25	115.257			
C5	103.81	111.087			
C6	103.28	111.008			
C17	79.99	82.288			
C16	77.48	77.748			
C15	57.71	65.922			

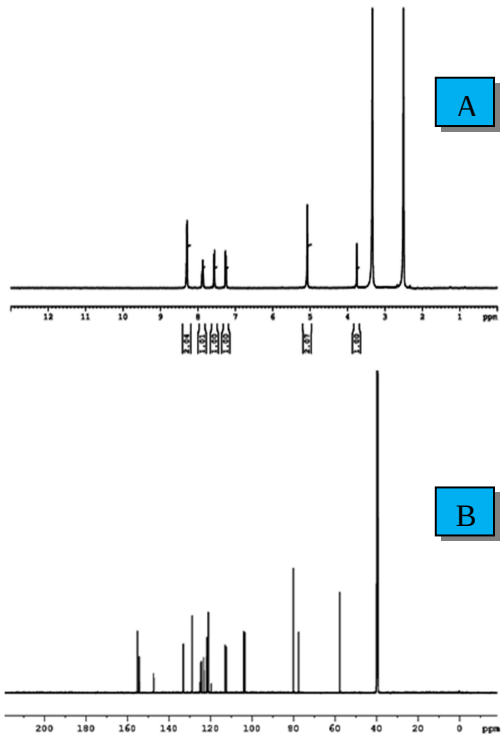

Fig.6. The experimental (A) ^{1}H NMR and (B) ^{13}C spectra of compound (**4**).

UV–vis spectrum and electronic properties

The electronic absorption spectra of the compound (**4**) in chloroform solvent were recorded within the 200 - 600 nm range and representative spectrum is shown in Fig. 5. As can be seen from the figure, electronic absorption spectra of this compound show three bands at 240, 333, and 341 nm. Electronic absorption spectra of compound (**4**) were calculated using the TD-DFT and TD-HF methods based on the B3LYP/6-31G(d) and HF/6-31G(d) level optimized structure in gas phase, respectively. For the TD-HF calculations, the absorption wavelengths are obtained at 157.95, 176.44, and 242.29 nm. It is obvious that these bands are not corresponding to the experimental results, which shows that to use TD-HF method here to predict the electronic absorption spectra is not reasonable. For TD-DFT calculations, the theoretical absorption bands are predicted at 199.72, 224.84 and 312.75 nm and it can easily be seen that they are corresponding to the experimental absorption ones. In addition to the calculations in gas phase, TD-DFT calculations of this compound in chloroform solvent were performed using the PCM model are obtained at 230 and 323 nm.

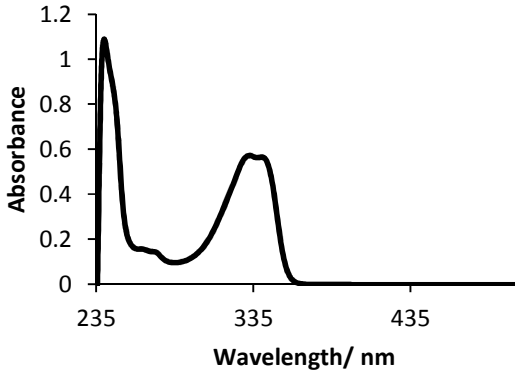

Fig. 7. UV-vis spectrum of the studied compound in chloroform solution.

The experimental and computed electronic values, such as absorption wavelength, excitation energies, frontier orbital energies, and oscillator strengths are tabulated in Table 4. The frontier orbitals are important in determining the electric and optical properties, as well as in UV–vis spectra and chemical reactions.[45, 46] Fig. 6 shows the distributions and energy levels of the HOMO-1, HOMO, LUMO and LUMO+1 orbitals computed at the B3LYP/6-31G(d) level for compound (**4**). From Fig. 6, the HOMO is mainly localized on the phthalonitrile ring and oxygen as well as cyano group. The LUMO are localized on phthalonitrile ring. The value of the energy separation between the HOMO and LUMO is 4.328 eV.

Table 4 Experimental and calculated wavelengths λ (nm), excitation energies (eV), oscillator strengths (*f*) and major contributions in chloroform solution for compound (4)

Exp. (in chloroform) λ (nm)	B3LYP/DFT (in chloroform) λ (nm)	Major contributions	E (eV)	*f*
240 333	230	H-3→L, H-2→L,H-1→L+2, H→L+3	5.400	0.7508
341	323	H→L, H-2→L+3	3.833	0.1889

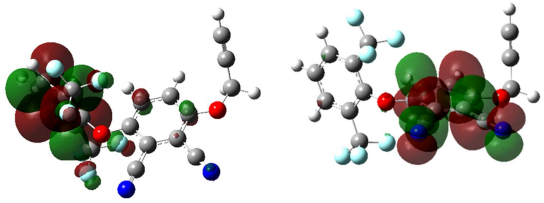

LUMO+1 (-1.379 ev) **LUMO (-2.318 ev)**

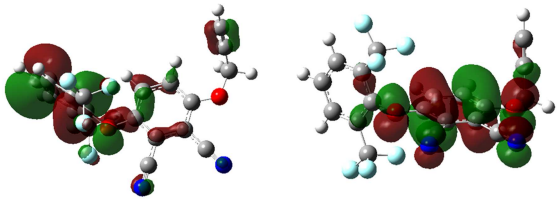

HOMO-1 (-7.661 ev) **HOMO(-6.646 ev)**

Fig. 8. Molecular orbital surfaces and energy levels using the DFT/B3LYP method for the, HOMO, HOMO–1, LUMO and LUMO + 1 of compound(**4**).

Molecular electrostatic potential maps

The MEP is related to the electronic density and is very important for describing and determining the sites for electrophilic and nucleophilic reactions as well as hydrogen bonding interactions.[47, 48] The importance of MEP is due to the displaying of molecular size, shape as well as positive, negative and neutral electrostatic potential regions in terms of color grading (Fig. 8a) and it is a very useful tool in research of molecular structure with its physiochemical property relationship. [49, 50] The negative regions (red and yellow) were related to electrophilic reactivity and the positive (blue) ones to nucleophilic reactivity.[51] The MEP at the B3LYP/ 6-31G(d) optimized geometry was calculated to predict the reactive sites for electrophilic and nucleophilic attack for the investigated molecule. The total electron density mapped with electrostatic potential surface and the electrostatic potential contour maps are shown in Fig. 8a and b, respectively. The different values of the electrostatic potential at the surface are represented by different colors. Potential increases in the order red < orange < yellow < green < blue. The color code of these maps is in the range between -0.05976 a.u (deepest red) to 0.05976 a.u (deepest blue) for the investigated compound. As can be seen from the figure, this molecule has two possible sites for electrophilic attack. Negative regions are mainly localized over the N1 and N2 atoms of the cyano groups while; the maximum positive region is localized on the C17-H17 bond, indicating a possible site for nucleophilic attack.

Click reaction

Placing terminal alkynyl group on phthalonitrile facilitate alkyne-azide click chemistry. The click reaction serves as a new approach for incorporation of a new functional group to get a new compound with new physical properties. With this approach, the original preparation of terminal-alkynylphthalonitrile was accomplished using the nucleophilic displacement reaction between 3-(2,6-bis(trifluoromethyl)phenoxy)-6-hydroxyphthalonitrile and propagyl bromide to give the target 'clickable' compound (**4**). Click reaction between terminal-alkynyl substituted phthalonitrile and (2-azidoethyl)-2,3,4,6-tetra-O-acetyl-β-D-glucopyranoside form triazole ring. The experimental evidence for this reaction is described as follow:

Accurate mass measurement

The resulting compound (**8**) from click reaction could be identified by means of exact mass measurement (Fig. 10). This compound shows a remarkable pattern.

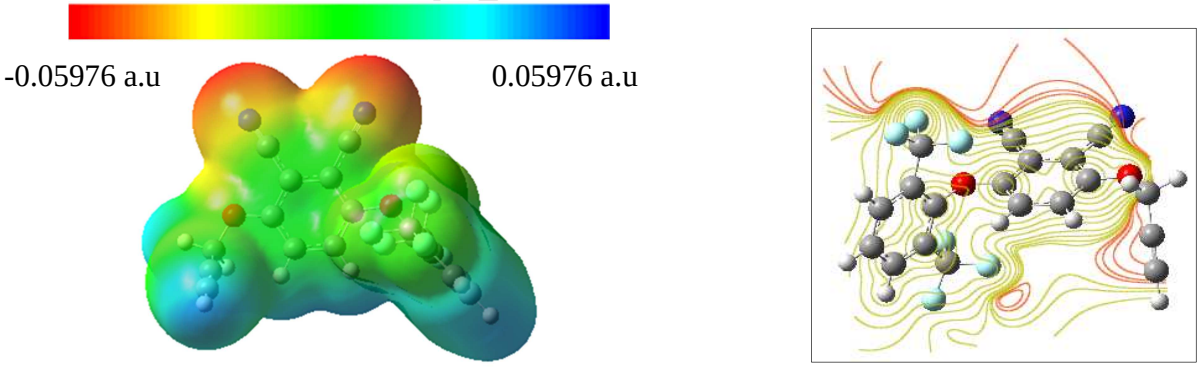

(a) **(b)**

Fig.9. (a) The total electron density mapped with electrostatic potential of compound (**4**). (b) The contour surface of electrostatic potential of compound (**4**).

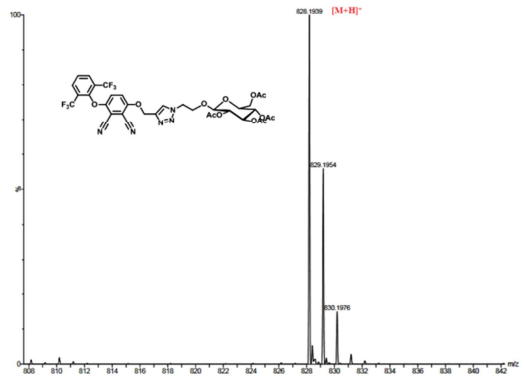

Fig. 10. ESI-Q-TOF product ion scans of **8** (m/z = 828.1939).

FT-IR and FT Raman measurements

The infrared and Raman spectra of this compound are compared in Fig. 11. FT-IR shows the presence of C≡N stretching vibration in the region at 2237.02 cm^{-1} and ester group at 1758.76 cm^{-1}. The FT Raman band found at 2237 and 1761.86 cm^{-1} due to the stretching vibration of C∋N and ester group, respectively.

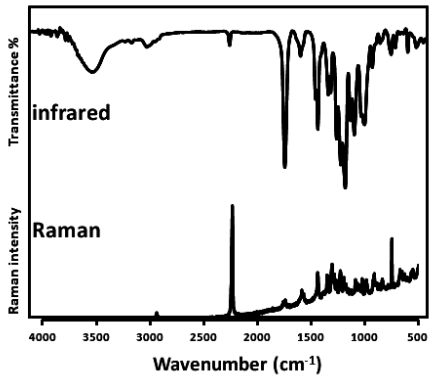

Fig. 11. Infrared and Raman spectra of compound (**8**)

^{1}H NMR measurements

As can be seen from fig. 12 is appearing the peak of H-triazole and acetylated sugar molecule.

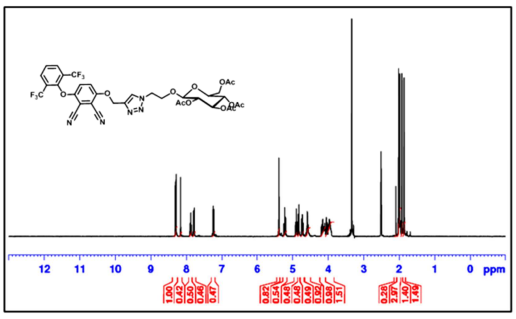

Fig. 12. ^{1}H NMR of compound (8).

Conclusion

In this paper, we designed fluorinated phthalonitrile with terminal alkyne grafted by carbohydrate azide as well as the theoretical studies on this fluorinated phthalonitrile with terminal alkyne compound by using the HF/6-31G(d) and DFT/B3LYP/6-31G(d) methods. A good agreement between experimental and calculated normal modes of vibrations has been observed. Grafting carbohydrates on to this precursor via click reaction offers several advantages for the resulting asymmetrical photosensitiser: besides the increasing possibility in the hydrophilicity for such compounds which aids delivery in aqueous systems, potential selective recognition and enhanced cell uptake by cancer cells for these species are possible.

Acknowledgement

The author acknowledges the support of this work by the Research Administration of Kuwait University, under the Grant Number SC02/14, the facilities of GFS (Chemistry Department, GS01/05, GS02/10, GS01/01, GS03/08, GS01/10 and GS01/03).

Reference

[1] PLASTICS AND COAL CHEMICALS DIVISION, Ind. Eng. Chem., 50 (1958) 92A–92A.
[2] C.C. Leznoff, and A. B. P. Lever, Phthalocyanines: Properties and Applications, VCH: New York, 1-4 (1989; 1993; 1996).
[3] K.M. Kadish, K. M. Smith and R. Guilard, The Porphyrin Handbook, Academic Press: California, 15-20 (2003).
[4] F. Lv, X He, li Lu, Li Wu and T. Liu, Synthesis, properties and near-infrared imaging evaluation of glucose conjugated zinc phthalocyanine via Click reaction, J Porphyrins Phthalocyanines, 16 (2012).
[5] A. Tuhl, Hacene Manaa, Saad Makhseed, Nouria Al-Awadi, Jacob Mathew, Hamada Mohamed Ibrahim, Tebello Nyokong and Haider Behbehani, Optical Materials 34 (2012) 1869–1877.
[6] T. Goslinski, and J. Piskorz, Fluorinated porphyrinoids and their biomedical applications, Journal of Photochemistry and Photobiology C: Photochemistry Reviews, 12 (2011) 304– 321.
[7] M. Meldal, and Christian Wenzel Tornøe, Cu-Catalyzed Azide-Alkyne Cycloaddition, Chem. Rev., 108 (2008) 2952–3015.
[8] C.W. Tornøe, and M. Meldal, Peptidotriazoles: Copper(I)-catalyzed 1,3- dipolar cycloadditions on solid-phase, Peptides, Proc. Am. Pept. Symp., (2001) 263-264.
[9] T. C. W. , C. Christensen, and M. Meldal Peptidotriazoles on solid phase: [1,2,3]-triazoles by regiospecific copper(i)-catalyzed 1,3-dipolar cycloadditions of terminal alkynes to azides, J Org Chem, 67 (2002) 3057–3064.
[10] V.V. Rostovtsev, L. G. Green , V. V. Fokin and K. B. Sharpless, A Stepwise Huisgen Cycloaddition Process: Copper(I)-Catalyzed Regioselective "Ligation" of Azides and Terminal Alkynes, Angew Chem Int Ed Engl, 41 (2002) 2596–2599.
[11] Y. Zorlu, Fabienne Dumoulin, Denis Bouchu, Vefa Ahsen and Dominique Lafont Monoglycoconjugated water-soluble phthalocyanines. Design and synthesis of potential selectively targeting PDT photosensitisers, 51 (2010) 6615–6618.
[12] H. Tanak, Yavuz Köysal, Şamil Işık, Hanifi Yaman and Vefa Ahsen, Experimental and Computational Approaches to

the Molecular Structure of 3-(2-Mercaptopyridine)phthalonitrile, Bull. Korean Chem. Soc., 32 (2011) 673- 680.
[13] M.D. Halls, R. Aroca, D. S. Terekhov, A. D'Ascanio and C. C. Leznoff, Vibrational spectra of halophthalonitriles, Spectrochimica Acta Part A: Molecular and Biomolecular Spectroscopy, 54 (1998) 305–317.
[14] H.M. Betül Nur Şen, Hatice Dinçer and Atıf Koca, Synthesis and characterization of terminalalkynyl-substituted unsymmetrical zinc phthalocyanine conjugated with well-defined polymers, Dyes and Pigments, 100 (2014) 1- 10.
[15] B. Furniss, A. Hannaford, P. Smith, and A. R. Tatchell, Vogel's Textbook of Practical Organic Chemistry, Longman Ltd., Harlow, UK, 5 th ed. (1989) 654.
[16] W. Hayes, H. M. I. Osborn, S. D. Osborne, R. A. Rastall and B. Romagnoli, One-Pot Synthesis of Multivalent Arrays of Mannose Mono- and Disaccharides, Tetrahedron, 59 (2003) 7983-7996.
[17] P.Y. Chong, and P. A .Petillo, Synthesis of carbamate-containing cyclodextrin analogues, Org. Lett., 2 (2000) 1093-1096.
[18] D. Wöhrle, M. Eskes, K. Shigehara and A. Yamada, A simple synthesis of 4,5-disubstituted benzenes and octasubstituted phthalocyanines, Synthesis, (1993) 194–196.
[19] H.B. Schlegel, Optimization of equilibrium geometries and transition structures, J. Comput. Chem. Rev., 3 (1982) 214-218.
[20] C. Peng, P. Y. Ayala, H. B. Schlegel and M. J. Frisch, Using redundant internal coordinates to optimize equilibrium geometries and transition states, J. Comput. Chem., 17 (1996) 49–56.
[21] M.J. Frisch, G. W. Trucks, H. B. Schlegel, G. E. Scuseria, M. A. Robb, J. R. Cheeseman, G. Scalmani, V. Barone, B. Mennucci, G. A. Petersson, H. Nakatsuji, M. Caricato, X. Li, H. P. Hratchian, A. F. Izmaylov, J. Bloino, G. Zheng, J. L. Sonnenberg, M. Hada, M. Ehara, K. Toyota, R. Fukuda, J. Hasegawa, M. Ishida, T. Nakajima, Y. Honda, O. Kitao, H. Nakai, T. Vreven, Jr. J. A. Montgomery, J. E. Peralta, F. Ogliaro, M. Bearpark, J. J. Heyd, E. Brothers, K. N. Kudin, V. N. Staroverov, R. Kobayashi, J. Normand, K. Raghavachari, A. Rendell, J. C. Burant, S. S. Iyengar, J. Tomasi, M. Cossi, N. Rega, N. J. Millam, M. Klene, J. E. Knox, J. B. Cross, V. Bakken, C. Adamo, J. Jaramillo, R, Gomperts, R. E. Stratmann, O. Yazyev, A, J. Austin, R. Cammi, C. Pomelli, J. W. Ochterski, R. L. Martin, K. Morokuma, V. G. Zakrzewski, G. A. Voth, P. Salvador, J. J. Dannenberg, S. Dapprich, A. D. Daniels, Ö. Farkas, J. B. Foresman, J. V. Ortiz, J. Cioslowski, and D. J. Fox, Gaussian 09, Revision B.01, Gaussian, Inc.: Wallingford, CT, USA, (2010).
[22] J.B. Foresman, and A. Frisch, Exploring Chemistry with Electronic Structure Methods, 2nd ed., Gaussian Inc., Pittsburgh, (1996).
[23] R. Dennington II, T. Keith and J. Millam, Gauss View Version 4.1.2, Semichem Inc., Shawnee Mission KS, (2007).
[24] E. Runge, and E. K. U. Gross, Density-Functional Theory for Time-Dependent Systems, Phys. Rev. Lett., 52 (1984) 997-1000.
[25] R.E. Stratmann, G. E.Scuseria and M. J. Frisch, An efficient implementation of time-dependent density-functional theory for the calculation of excitation energies of large molecules, J. Chem. Phys., 109 (1998) 8218.
[26] R. Bauernschmitt, and R. Ahlrichs, Treatment of electronic excitations within the adiabatic approximation of time dependent density functional theory, Chem. Phys. Lett., 256 (1996) 454-464
[27] M.E. Casida, C. Jamorski, K. C. Casida, D. R. Salahub Molecular excitation energies to high-lying bound states from time-dependent density-functional response theory: Characterization and correction of the time-dependent local density approximation ionization threshold, J. Chem. Phys. , 108 (1998) 4439-4449.
[28] S. Miertus, E. Scrocco and J. Tomasi Electrostatic Interaction of a Solute with a Continuum. A Direct Utilization of ab Initio Molecular Potentials for the Prevision of Solvent Effects, J. Chem. Phys., 55 (1981) 117-129.
[29] V. Barone, and M. Cossi, Quantum Calculation of Molecular Energies and Energy Gradients in Solution by a Conductor Solvent Model, J. Phys. Chem. A, 102 (1998) 1995-2001.
[30] J. Tomasi, B. Mennucci and R. Cammi, Quantum mechanical continuum solvation models, Chem. Rev., 105 (2005) 2999-3093.
[31] R.M. Ditchfield, J Chem Phys, 56:5688 (1972).
[32] K. Wolinski , James F. Hinton and Peter Pulay, Efficient implementation of the gauge-independent atomic orbital method for NMR chemical shift calculations, J. Am. Chem. Soc., 112 (1990) 8251–8260.
[33] P. Murray-Rust, W.C. Stallings, C.T. Monti, R.K. Preston and J.P. Glusker, Intermolecular interactions of the carbon-fluorine bond: the crystallographic environment of fluorinated carboxylic acids and related structures, J. Am. Chem. Soc. , 105 (1983) 3206-3214.
[34] J.A.R.P. Sarma, and G. R. Desiraju, Acc. Chem. Res., 19 (1986) 222- 228.
[35] S.L. Price , A. J. Stone , J. Lucas , R. S. Rowland and A. E. Thornley, The Nature of -Cl.cntdot..cntdot..cntdot.Cl-Intermolecular Interactions, J. Am. Chem. Soc., 116 (1994) 4910–4918.
[36] N. Ramasubbu, R. Parthasarathy and P. Murrayrust Angular Preferences of Intermolecular Forces around Halogen Centers—Preferred Directions of Approach of Electrophiles and Nucleophiles around the Carbon Halogen Bond, J. Am. Chem. Soc. , 108 (1986) 4308–4314.
[37] G. Desiraju, and R. Parthasarathy, The nature of halogen.cntdot..cntdot..cntdot.halogen interactions: are short halogen contacts due to specific attractive forces or due to close packing of nonspherical atoms?, J. Am. Chem. Soc., 111 (1989) pp 8725–8726.
[38] L. Shimoni, H. L. Carell, J. P. Glusker and M. M. Coombs, Intermolecular Effects in Crystals of 11-(Trifluoromethyl)-15,16-dihydrocyclopenta[a]phenanthren-17-one, J. Am. Chem. Soc., 116 (1994) 8162–8168.
[39] L. Pauling, The Nature of the Chemical Bond, 3rd ed., Cornell University Press: Ithaca, NY, (1960).
[40] D. Chopra , T. S. Cameron , Joseph D. Ferrara , and Tayur N. Guru Row, Pointers toward the Occurrence of C–F···F–C Interaction: Experimental Charge Density Analysis of 1-(4-Fluorophenyl)-3,6,6-trimethyl-2-phenyl-1,5,6,7-tetrahydro-4H-indol-4-one and 1-(4-Fluorophenyl)-6-methoxy-2-phenyl-1,2,3,4-tetrahydroisoquinoline, J. Phys. Chem. A, 110 (2006) 10465–10477.
[41] N. Sundaraganesan, S. Ilakiamani, H. Saleem, P.M. Wojciechowski and D. Michalska, FT-Raman and FT-IR spectra, vibrational assignments and density functional studies of 5-bromo-2-nitropyridine, Spectrochim. Acta A Mol. Biomol. Spectrosc., 61 (2005) 2995-3001.
[42] A. Teimouri, A. N. Chermahini, K. Taban and H. A. Dabbagh Experimental and CIS, TD-DFT, ab initio calculations of visible spectra and the vibrational frequencies of sulfonyl azide-azoic dyes, Spectrochim. Acta Part A Mol Biomol Spectrosc, 72 (2009) 369-377.

[43] A.P. Scott, and Leo Radom Harmonic Vibrational Frequencies: An Evaluation of Hartree–Fock, Møller–Plesset, Quadratic Configuration Interaction, Density Functional Theory, and Semiempirical Scale Factors, J. Phys. Chem., 100 (1996) 16502–16513.
[44] A. Teimouri, M. Emami, A. N. Chermahini and H. A. Dabbagh, Spectroscopic, quantum chemical DFT/HF study and synthesis of [2.2.1] hept-2'-en-2'-amino-N-azatricyclo [3.2.1.0(2,4)] octane, Spectrochim Acta A Mol Biomol Spectrosc, 71 (2009) 1749-1755.
[45] H. Tanak, Quantum chemical computational studies on 2-methyl-6-[2-(trifluoromethyl)phenyliminomethyl]phenol, J. Mol. Struct.: THEOCHEM, 950 (2010) 5-12.
[46] I. Fleming, Frontier Orbitals and Organic Chemical Reactions, Wiley, London, (1976).
[47] E. Scrocco, and J. Tomasi, Electronic Molecular Structure, Reactivity and Intermolecular Forces: An Euristic Interpretation by Means of Electrostatic Molecular Potentials, Advances in Quantum Chemistry, 11 (1978) 115–193.
[48] F.J. Luque, J. M. López and M. Orozco, Perspective on "Electrostatic interactions of a solute with a continuum. A direct utilization of ab initio molecular potentials for the prevision of solvent effects", Theor. Chem. Acc. , 103 (2000) 343-345.
[49] J.S. Murray, and K. Sen, Molecular electrostatic potentials : concepts and applications, Amsterdam: Elsevier, (1996).
[50] E. Scrocco, and J. Tomasi, Advances in Quantum Chemistry, P. Lowdin, Ed., Academic Press, New York, NY, USA, (1978).
[51] P. Politzer, and D. G. Truhlar, Chemical Applications of Atomic and Molecular Electrostatic Potentials, Plenum Press, New York, (1981) 1-6.

Highlights

- The spectroscopic properties of the compound were investigated by DFT method.
- The DFT theoretical results were compared experimental results.
- Click reaction between terminal-alkynyl substituted phthalonitrile and (2-azidoethyl)-2,3,4,6-tetra-O-acetyl-β-D-glucopyranoside to form triazole ring.